1

Introduction to Metal Nanocluster Catalysis

1.1 Catalysis and Metal Catalysts

Chemical reactions provide a way to create new molecules, which have been widely used in our lives. The energy difference between reactants and products gives driving force for the chemical reactions. However, in general, these reactions cannot happen directly because of the existence of intermediates (or transition states) which bear higher Gibbs energy than the reactants. To promote the smooth progress of reactions, catalysts are needed to significantly reduce the reaction energy barrier between the intermediate (or transition state) and the reactant (Figure 1.1). The catalysts-promoted chemical reactions can be called catalytic process, that is, catalysis. More than 80% of chemical reactions involve catalysis. Among of them, metal species-promoted catalytic processes play important roles in the construction of functional molecules [1–7], which are difficult to be obtained in other ways. Almost half of Nobel Prizes in Chemistry are directly or indirectly relevant to metal catalysis. Typical examples include the "click chemistry and biorthogonal chemistry" (2022), "palladium-catalyzed cross couplings in organic synthesis" (2010), "metathesis method in organic synthesis" (2005), "chirally catalyzed hydrogenation and oxidation reactions" (2001), etc.

Generally, metal catalysts activate molecules in three ways. First, σ-donation and π-backdonation process (Figure 1.2a). Taking the nitrogen gas (N_2) activation as an example, a number of transition metals have been found to be able to bind N_2 by the mode of σ-donation and π-backdonation [8]. This N_2 activation mode was found since the discovery of the Haber–Bosch process. This kind of catalytic activity of metals is attributed to their advantageous combination of unoccupied and occupied d orbitals, which are of appropriate energy and symmetry to synergistically accept electron density from and backdonate to N_2. The σ-donation and π-backdonation process highly weakens the nitrogen–nitrogen triple bond while simultaneously strengthening the metal–nitrogen bond, thus endowing metals with catalytic activity toward N_2 and other molecules such as alkenes, alkynes, etc.

Metal Nanocluster Catalysis: From Fundamentals to Applications, First Edition. Manzhou Zhu and Man-Bo Li. Published 2026 by Wiley-VCH GmbH.

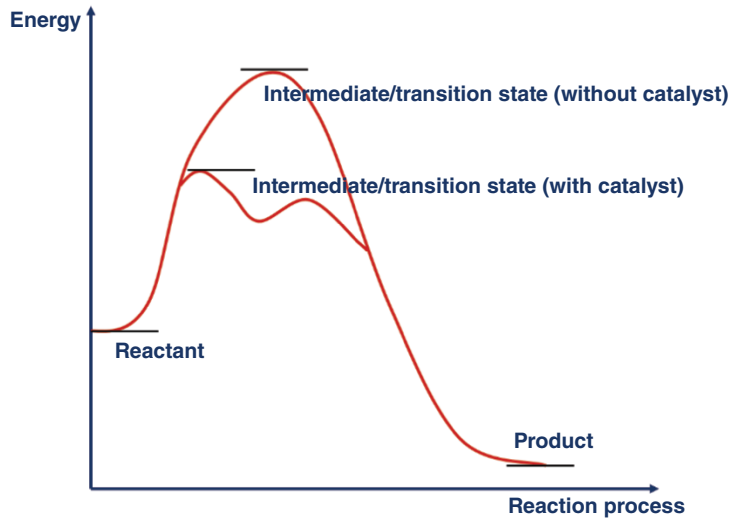

Figure 1.1 Illustration of catalytic process.

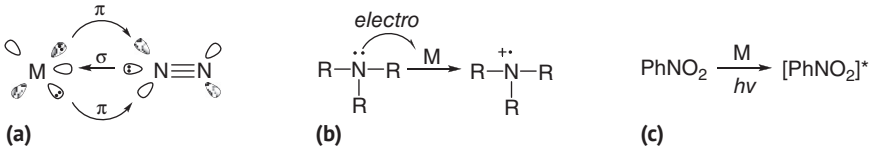

Figure 1.2 Three catalytic modes of metal catalysts.

Second, electron transfer process (Figure 1.2b). Taking the trialkyl amine activation as an example, metals bearing abundant valence states are generally able to undergo electron transfer process. Under the conditions of electrolysis or light irradiation, one of the lone pair electrons on the trialkyl amine would be abstracted by the metal, thus generating the trialkyl amine radical cation [9]. This species is quite active and can be further transformed to carbon radicals or captured directly by other molecules. The as-formed radical intermediates abstract an electron from the reduced metal, giving M and finishing the catalytic cycle. Third, energy transfer process (Figure 1.2c). Taking the nitrobenzene activation as an example, photosensitive metal species are usually capable of energy transfer process. The photosensitive metal catalyst would be excited under light irradiation, giving the excited state metal catalyst. This active species contacts with nitrobenzene in the reaction system. Energy transfer between the excited metal catalyst and nitrobenzene would regenerate metal catalyst and produce activated nitrobenzene [10], which can be further transformed in the presence of other organic molecules. Sometimes the metal catalyst interacts with molecules and forms the metal-molecule complex that is more easily excited and undergoes intracomplex energy transfer process under light irradiation.

The three catalytic modes are involved in various metal catalysts including metal salts, metal-ligand chelates, metal nanoclusters, metal nanoparticles, metal–organic frameworks, etc. The content in the following sections and chapters will also focus on the three catalytic modes, introducing different reactions catalyzed by metals.

1.2 Single Metal Atom, Metal Nanocluster, and Metal Nanoparticle

From the size point of view, the common metal catalysts can be divided into the following three types: single metal atoms, metal nanoclusters and metal nanoparticles (Figure 1.3). For single metal atoms, their sizes range from 0.5 to 2.5 Å. For the roles of controlling catalytic activity and selectivity, the single metal atom can be surrounded by inorganic/organic carriers, counter ions, or organic ligands. Therefore, the true size of single metal atom catalysts is dramatically larger than the diameters of metal atoms, probably reaching to 1 nm. Metal nanoclusters composed of several metal atoms generally fall in the range of 1–3 nm. The bare metal nanoclusters are quite active because of their high surface energy. They are stabilized by either organic ligands or carriers, which help to reduce the surface energy and regulate catalytic activity and selectivity of the metal kernel as well. Generally speaking, the metal nanocluster is a group of metal atoms that are connected by metal–metal or metal–organic interactions [11, 12]. They have relatively blurring boundaries with metal nanoparticles. On the other hand, it should be clarified that the narrowly defined metal nanocluster is the metal aggregate possessing direct metal bonding interactions, well-defined composition and atomically precise structure [13–15]. Metal nanoparticle has been widely used currently in various subjects such as chemistry, materials, physics, biology, and information. It has a metal kernel with size ranging from several to tens and hundreds of nanometers, and even to micrometers. Inorganic or organic layers are surrounded on the surface to protect the metal kernel from aggregation or decomposition. Metal nanoclusters and nanoparticles have distinct physicochemical properties compared to single metal atoms. The 2023 Nobel Prizes in Chemistry "discovery and synthesis of quantum dots" displays the unique properties of this kind of material.

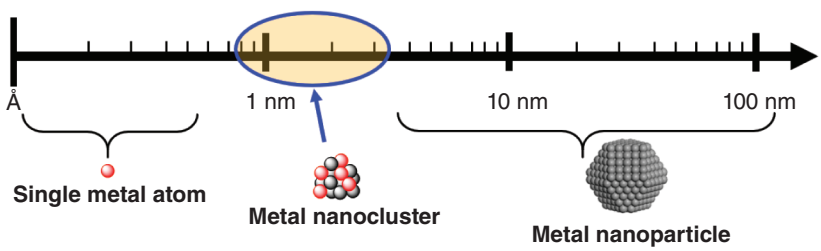

Figure 1.3 The size of single metal atom, metal nanocluster, and metal nanoparticle.

From the catalytic property point of view, single metal atom has the most surface metal atoms, that is, the potential activation sites. Nowadays, the most frequently used metal catalysts are homogeneous single metal atom catalyst [16–19], such as metal salts and metal chelates. Each metal site contacts with reactants sufficiently under homogeneous reaction conditions, triggering high catalytic activity and selectivity. It should be noted that for certain metals, their homogeneous single atom forms with different valence states have significantly different catalytic activities. We are merely citing Pd catalysis as a typical example (Figure 1.4). The single Pd^0 atom catalyst such as $Pd(PPh_3)_4$ has been found to be highly active to the cross-coupling process [20]. The low-valence-state palladium would be oxidized by the aryl-halide, generating the Pd^{II} intermediate via an elementary reaction of oxidative addition. This intermediate can be trapped by an organometallic reagent and transformed to the other Pd^{II} intermediate via an elementary reaction of transmetallation. The as-obtained Pd^{II} intermediate undergoes the third elementary reaction of reductive elimination, furnishing the final cross-coupling product and regenerating the Pd^0 catalyst. The single Pd^{II} atom catalyst such as $PdCl_2$ demonstrates a dramatically distinct catalytic activity compared to the Pd^0 species. A typical example is the Pd^{II}-catalyzed Wacker process [21]. The high-valence-state palladium prefers coordinating with electron-rich compounds such as the alkene. The activated alkene would be attacked easily by a nucleophile such as H_2O, producing a Pd^{II} intermediate via an elementary reaction of olefin insertion. The following elementary reaction of β-H elimination would give the aldehyde as the final product and produce Pd^0 species, which is oxidized to regenerate the Pd^{II} catalyst. The significantly different catalytic processes shown in Figure 1.4 represent the catalytic difference of single metal atoms with different valence states, which have been widely applied in pharmaceutical industry and acetaldehyde production, respectively.

Apart from the homogeneous single metal atom catalysts, heterogeneous single metal atom catalysts [22–25] have shown exceptional catalytic performance in recent years. They are composed of single metal atoms that are anchored on different carriers to reduce the high surface energy. The carriers around metal atoms play the similar role with the organic ligands of metal chelates, on the one hand stabilizing

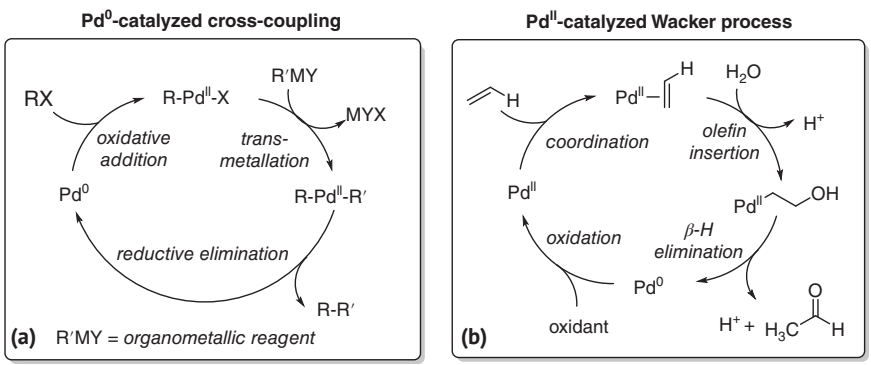

Figure 1.4 Typical examples on single Pd^0 (a) and Pd^{II} (b) atom catalysis.

the metal center and on the other hand facilitating control of catalytic activity and selectivity. Additionally, the heterogeneous single metal atom catalysts are readily recovered from the catalytic reactions by simple procedures such as centrifugation and then recycled, thus being highly beneficial for industrial applications.

Being different from the carrier-supported heterogeneous single metals, metal nanoparticles [26–28] are self-supported heterogeneous metal catalysts. They are usually composed of a metal kernel and an organic surface. Besides their advantage of recoverability and recyclability during catalysis, the catalytic synergy among different activation sites on the surface endows metal nanoparticles with different activity and selectivity compared to single metal atom catalysts. Molecular adsorption and desorption should be well considered for metal nanoparticle catalysis because both processes are rate-determining steps in many cases [29].

As a result of the significantly different catalytic mechanisms between metal nanoparticle catalysis and single metal atom catalysis, they exhibit distinct catalytic selectivity even if the metal and ligand types are the same, respectively. We still take the palladium catalysis as a typical example. Pd^{II}-catalyzed oxidative carbocyclization reactions constitute an efficient route to diverse cyclic carbon compounds. The group of Jan-E Bäckvall developed a series of Pd^{II}-catalyzed oxidative carbocyclizations of allenes via a key process of allenic C(sp^3)-H bond oxidation [30–33]. Recently, Jan-E Bäckvall and Man-Bo Li found that replacement of the single palladium atom catalyst ($Pd(OAc)_2$) by the palladium nanoparticle catalyst (1–2 nm palladium nanoparticles immobilized on amino-functionalized siliceous mesocellular foam) gave completely different selectivities for the catalyzed oxidative carbocyclizations (Figure 1.5) [34]. Specifically, for the oxidative carbocyclization-alkynylation of enallenes with a —OH substituent, the palladium nanoparticle gave the desired product with high yield and diastereoselectivity while $Pd(OAc)_2$ catalyzed the reaction and produced an oxidative carbocyclization product. A β-hydride elimination instead of alkynylation should be attributed to the different selectivity of $Pd(OAc)_2$ catalysis. Control experiments further revealed that the Pd-amine synergy on the surface of the palladium nanoparticle promoted the alkynylation of the palladium intermediates, thus affording the oxidative carbocyclization-alkynylation product with high efficiency (Figure 1.5a).

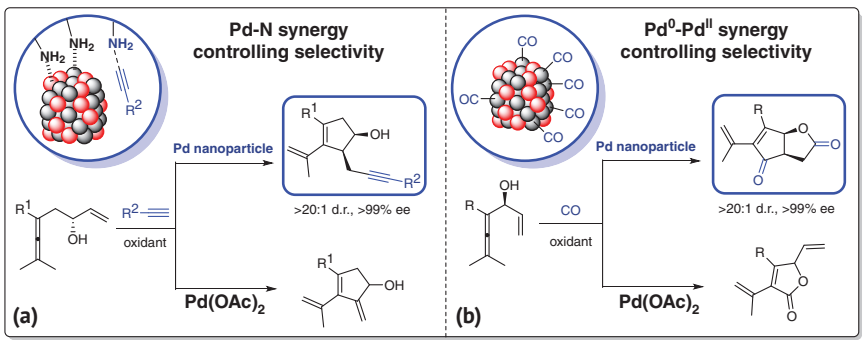

Figure 1.5 Pd-N and Pd-Pd synergy for palladium nanoparticle catalysis.

Apart from the Pd-N synergy, the Pd^0-Pd^{II} synergy on the surface of palladium nanoparticles also triggers selectivity switching of oxidative carbocyclization of allenes. As shown in Figure 1.5b, compared to Pd^{II}, Pd(0) atoms favor adsorption and coordination of CO, thus resulting in the aggregation of CO in the palladium nanoparticle catalyst. The local high CO concentration would promote the generation a subsequent carbocyclization to give the bicyclic compound as the final product (Figure 1.5b). In sharp contrast, $Pd(OAc)_2$-catalyzed reaction gave the monocyclic compound as the product because of the unfavored second carbonylation process. The distinct selectivity of metal nanoparticle-catalysis, combined with their recoverability and recyclability after catalysis, would be highly promising for their practical applications in industrial catalysis.

Being similar with metal nanoparticles, metal nanoclusters are metal aggregates stabilized by inorganic or organic species. As mentioned above, metal nanoclusters fall in the gap between single metal atoms and metal nanoparticles. They can be considered as the nascent states during the aggregation of metal atoms to metal nanoparticles. Therefore, they are usually more active than the stabilized metal nanoparticles, possessing promising catalytic potentials. Actually, in many metal-catalyzed transformations, the real catalysts are the in situ generated metal nanoclusters. They are formed either by bottom-up process from single metal atoms under homogeneous catalytic conditions or top-down process from metal nanoparticles under heterogeneous catalytic conditions. However, this kind of special species is highly active and difficult to be isolated and characterized. This part will be discussed in detail in the next chapter "In situ generated metal nanocluster catalysis" of the book. The main challenge of research of metal nanocluster catalysis is stabilize these highly active species while keeping them catalytically active. A stable and characterizable structure is the prerequisite for in-depth investigation of their unique catalytic activity, selectivity, and mechanism. Carriers or organic ligands are generally employed to support or protect the metal kernels, thus stabilizing metal nanoclusters for catalytic investigations. The stabilized metal nanoclusters that enable isolation and characterization after catalysis will be discussed in detail in Chapter 3 "Supported metal nanocluster catalysis" and Chapters 4–6 "Organic ligand protected metal nanocluster catalysis" of the book.

It should be noted that the single metal atom, metal nanocluster, and metal nanoparticle can be transformed reversibly in certain reaction conditions (Figure 1.6) [35, 36]. The aggregation of metal atoms would result in the generation of metal nanoclusters and even metal nanoparticles. On the other hand, metal leaching on

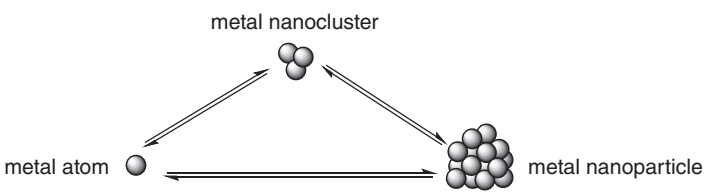

Figure 1.6 Mutual transformation among the single metal atom, metal nanocluster, and metal nanoparticle during catalysis.

the surface of nanoparticles lead to the formation of metal atoms or metal nanoclusters in the reaction solutions. The idea of the aggregation and leaching processes has been discussed in many reports. For instance, the palladium leaching process (the formation of soluble metal species from palladium black) was discussed by Mizoroki in the early seventies, just after the first examples of Pd-catalyzed Mizoroki–Heck reaction had been published. The interconversion of various metal species during catalytic reactions have governed the development of the concept of a "Cocktail" of metal catalysts, which facilitate catalytic reactions such as the cross-coupling reaction, hydrogenation, C—H functionalization, etc. for a broad range of substrates. Meanwhile, the mutual transformation and coexistence of single metal atoms, metal nanoclusters, and metal nanoparticles would result in an ambiguous mechanism and raise the arguments on the topic of "What is the true catalyst?" In-depth mechanistic investigations including the kinetics will be helpful to clarify the true active species even though the catalytic reactions are dynamic and nothing can be static in catalysis.

1.3 Metal Nanocluster Catalysis: Activity

The highly catalytic activity of metal nanocluster catalysis would be the first feature comes into one's mind. In earlier research on metal nanocluster catalysis, it has been reported that metal nanoclusters demonstrated significantly higher catalytic activity than other metal species. For example, Huang and coworkers prepared gold nanocluster (<2.0 nm) deposited on alkaline-treated titanosilicalite by solid grinding with dimethyl gold acetylacetonate [37]. They further found that this nanocluster catalyst triggered the transformation from the propene to the propene epoxide with the metal time yield of 2.3 $g_{PO}g^{-1}{}_{Au}h^{-1}$. The propene conversion and selectivity were determined to be near 1.0% and above 50%, respectively. Although this catalytic performance is not sufficiently high for an industrial application, it is much better than those of general copper- and silver-based catalysts utilized for this reaction (Table 1.1).

In another report from Turner and coworkers [38], a sharp size threshold of nanogold catalysts was found for styrene oxidation. A series of nanogold with different sizes were synthesized and located on the titanium dioxide (110) single crystal. Only when the size falls below about 3.5 nm, the nanogold catalysts were catalytically active. Especially, the gold nanocluster composed of 55 gold atoms (~1.4 nm) was found to be an efficient and robust catalyst for the selective oxidation of styrene by dioxygen (Table 1.2). This typical case unambiguously indicates the high catalytic activity of metal nanoclusters compared to metal nanoparticles.

The high activity of metal nanoclusters was discovered not only in oxidation reactions but also in C—C cross-coupling reactions. Reetz and de Vries found that activated and nonactivated aryl bromides underwent smooth ligand-free Heck reactions [39], featuring low amounts of palladium salts such as $Pd(OAc)_2$ (ideally 0.01–0.1 mol%). Experimental results such as the in situ transmission electron microscopy (TEM) demonstrated that this industrially viable process appears to involve palladium

Table 1.1 Oxidation of C_3H_6 with O_2 in the presence of H_2O by gold catalysts.[a]

Support	Au loading [wt%][b]	Pretreatment atmosphere,[c] temperature [K]	Au nanocluster diameter [nm][d]	Conv. of C_3H_6 [%]	Selectivity of propene epoxide [%]
Titanosilicalite	0.19	H_2, 423	4.6	0.07	0
Titanosilicalite	0.19	H_2, 423	1.8	0.88	52
Titanosilicalite	9.0[e]	H_2, 473	—	0.47	57
γ-Al_2O_3	0.86	Air, 573	2.6	0.15	0
Al_2O_3 (amorphous)	0.19	H_2, 423	<2.0[f]	0.15	0
TiO_2	1.2	Air, 573	2.9[f]	0.03	0
TiO_2	0.10	Air, 573	1.8	0.05	0

a. Reaction conditions: catalyst 0.3 g; reaction temperature 473 K (for Au/TiO_2, 353 K); feed gas $C_3H_6/O_2/H_2O/Ar = 10/10/2/78$; space velocity 4000 $mL g^{-1}_{cat.}\ h^{-1}$. Data were taken under a steady state after at least 2-hour duration.
b. Actual Au loadings obtained by inductively coupled plasma (ICP) analysis.
c. H_2 (10 vol%) was diluted by 90 vol% Ar.
d. The diameters of gold nanoclusters determined by HAADF-STEM observation after catalytic tests.
e. Gold loading calculated from the gold content in the starting solution.
f. The diameters of gold nanoparticles or clusters determined by TEM observation after catalytic tests. Over Au/amorphous Al_2O_3, because no Au particles could be found by TEM, the diameter was estimated to be smaller than 2.0 nm.

Table 1.2 Catalytic results of oxidation of styrene using O_2 alone for different Au catalysts.

Catalyst	Au loading [wt%]	Au nanocluster/ particle diameter [nm]	Conversion [%]	Selectivity of styrene epoxide [%]
Au_{55}/BN	0.63	1.6	19.2	14.0
Au_{55}/SiO_2	0.67	1.5	25.8	12.0
Au_{55}/SiO_2 recycled 1	0.67	—	21.4	23.7
Au_{55}/SiO_2 recycled 2	0.67	—	15.9	27.1
Au/SiO_2	6.35	3.0	Trace	—
Au/SiO_2	0.60	4.0	Trace	—
Au/C	1.0	17.0	No reaction	—
Au/SiO_2	5.0	>30	No reaction	—

nanoclusters with the size of approximately 1.6 nm. Leyva-Perez and coworkers further investigated the active catalytic species in ligand-free C—C cross-coupling reactions [40], such as Heck, Sonogashira, Suzuki, and Stille coupling reactions. By using TEM together with dynamic light scattering (DLS) measurements, it was confirmed that the palladium atoms aggregated to form 2–10 nm palladium nanoparticles in a few minutes when the reaction was carried out. However, the reaction-induction

period continued for approximately two additional hours after the formation of the palladium nanoparticles. The result unambiguously indicates that the palladium nanoparticles generated in situ are not the catalytically active metal species. Furthermore, they analyzed reaction samples before and after the induction time by electrospray ionization mass spectrometry (ESI-MS) and matrix-assisted laser desorption/ionization coupled to time-of-flight (MALDI-TOF) mass spectrometry. Results showed that the C—C coupling reactions initiated on when palladium nanoclusters with a mass below 500 Da appear. Based on the jellium model, significant emission signals (450 nm) were only observed in the range of 336–370 nm, which corresponds to small clusters with three and four metal atoms. This real catalytic species was observed to be partially stabilized by water in the reaction system, and demonstrated turnover frequencies (TOFs) between 10^5 and 10^6 molecules of product per atom of palladium per hour. Ellis and coworkers found the similar catalytic performance of in situ generated palladium nanoclusters and provided the direct evidence that the Suzuki coupling reaction can occur heterogeneously at the surface of polyvinylpyrrolidone (PVP)-stabilized palladium nanoclusters with the help of a combination of operando X-ray absorption spectroscopy (XAS), surface sensitive X-ray photoelectron spectroscopy (XPS), and detailed kinetic profiling [41].

Being different from the closest packing of metal atoms in bulk metal catalysts, for example, face-centered cubic (fcc) for gold, body-centered cubic (bcc) for ferrum and hexagonal close-packed (hcp) for cobalt, the packing style of metal atoms in metal nanoclusters are much more diverse. Therefore, not all metal nanoclusters are active in catalysis. The catalytic activities of metal nanoclusters are highly dependent on the metal atom packing style. A recent report from Ruan and coworkers indicates that palladium nanoclusters with the same composition $Pd_6(SR)_{12}$ but different metal atom packing styles exhibit different catalytic activities in Sonogashira coupling reaction and 4-nitrophenol reduction reaction (Figure 1.7) [42]. The $Pd_6(SR)_{12}$ nanocluster with tiara-like structure (Pd6-Tia) is more active than the $Pd_6(SR)_{12}$ nanocluster with octahedral structure (Pd6-Oct) during catalysis. Pd6-Tia displayed 100% selectivity and 90% catalytic yield for the Sonogashira coupling between iodobenzene and phenylacetylene, while Pd6-Oct catalyzed the reaction under the same

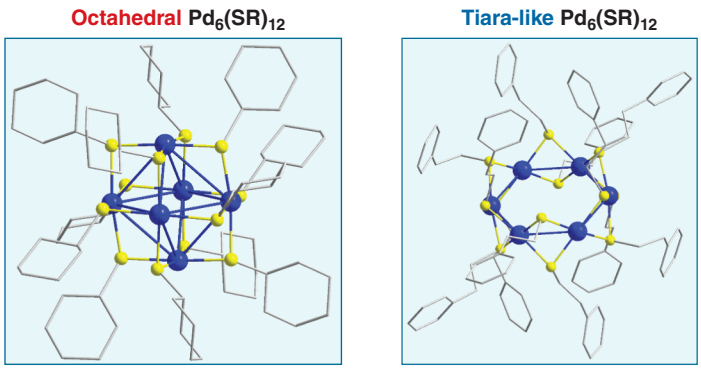

Figure 1.7 Pd_6 nanoclusters with different metal atom packing styles.

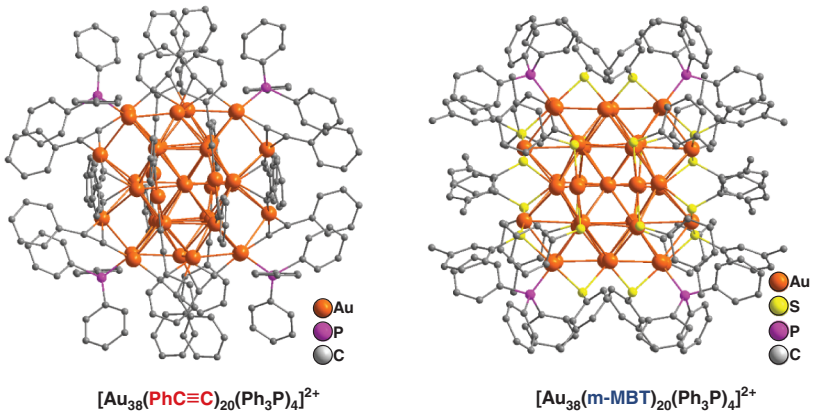

Figure 1.8 Au_{38} nanoclusters with different surrounding ligands.

conditions with only 24% yield. For the hydrogenation of 4-nitrophenol, the reaction rate constant with Pd6-Tia is significantly higher than that with Pd6-Oct.

The ligand surrounds the metal kernel is another key factor that impact the catalytic activity of metal nanoclusters. Wan and coworkers synthesized two isostructural Au_{38} nanoclusters $[Au_{38}L_{20}(PPh_3)_4]^{2+}$, in which L is alkynyl and thiolate groups for the two nanoclusters, respectively (Figure 1.8). Both Au_{38} nanoclusters possess an fcc gold kernel. However, they displayed completely different catalytic activities toward the semihydrogenation of alkynes [43]. $\left[Au_{38}\,(PhC{\equiv}C)_{20}\,(PPh_3)_4\right]^{2+}$ nanocluster with the alkyne ligand catalyzed the hydrogenation of terminal and internal alkynes, giving the corresponding alkenes with nearly 100% conversion and selectivity. In sharp contrast, $[Au_{38}(SR)_{20}(PPh_3)_4]^{2+}$ (SR = 3-methylbenzenethiol, m-MBT) nanocluster with the thiolate ligand was catalytically inert toward the terminal alkynes as well as the internal alkynes.

The potentially high and adjustable catalytic activities not only endow metal nanoclusters with interesting catalytic properties for fundamental research but also provide a kind of dominant metal catalyst that has promising catalytic performance in industrial applications. In the next chapters, we will discuss their diversified activities in various catalytic reactions.

1.4 Metal Nanocluster Catalysis: Selectivity

As we have mentioned in Section 1.2, metal nanoparticles present different catalytic selectivity compared with the single metal atom catalysts in some cases because of the metal–metal synergy on the surface of metal nanoparticles. Similarly, metal nanoclusters catalyzed reactions, giving different selectivity with single metal atoms as well. Pun and coworkers found an interesting phenomenon when they were studying the aerobic dehydrogenation of cyclohexanone by palladium catalysts (Figure 1.9) [44]. When $Pd(DMSO)_2(TFA)_2$ (DMSO = dimethylsulfoxide;

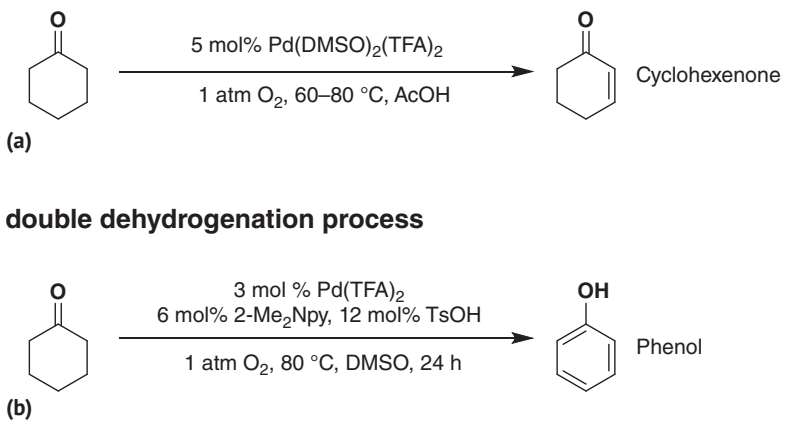

Figure 1.9 Switched catalytic selectivity of Pd-catalyzed cyclohexanone dehydrogenation.

TFA = trifluoroacetate) was applied as the palladium catalyst, the reaction stopped at the first stage and gave the single dehydrogenation cyclohexenone as the final product. When $Pd(TFA)_2$/2-dimethylaminopyridine (2-Me_2Npy) was applied as the palladium catalyst, the reaction favored a second dehydrogenation and afforded the phenol as the final product. They envisioned that different catalytic species were involved with $Pd(DMSO)_2(TFA)_2$ and $Pd(TFA)_2$/2-Me_2Npy catalytic system, respectively. DLS, TEM, and kinetic studies all suggested that palladium nanoclusters were formed under the reaction conditions using $Pd(TFA)_2$/2-Me_2Npy. The as-obtained palladium nanoclusters are much active than the Pd^{II} species in catalyzing the conversion from cyclohexanone to phenol, thus triggering the double dehydrogenation of cyclohexanone. Under the reaction conditions using $Pd(DMSO)_2(TFA)_2$, DMSO efficiently protects the Pd^{II} species from aggregation [45] and holds the reaction at the single dehydrogenation stage. The distinct catalytic selectivity between the single palladium atoms and the palladium nanocluster should be ascribed to their different valence state, redox capability, and dehydrogenation pathways.

Similarly, Fricke and coworkers found an interesting experimental result [46], that is, aryl germanes are unreactive in single palladium atom $LnPd^0/LnPd^{II}$ catalysis and allow selective functionalization of established coupling partners in their presence. On the contrary, they display superior reactivity under palladium nanocluster conditions, outcompeting established coupling partners such as ArBPin and allowing air-tolerant, base-free, and orthogonal access to valuable and challenging diaryl motifs. The single palladium atoms and palladium nanoclusters conditions can be achieved, respectively, by using or not using phosphine ligands with palladium salts. Based on the different catalytic selectivity of single palladium atoms and palladium nanoclusters, they developed an orthogonal catalysis strategy with organogermanes (Figure 1.10).

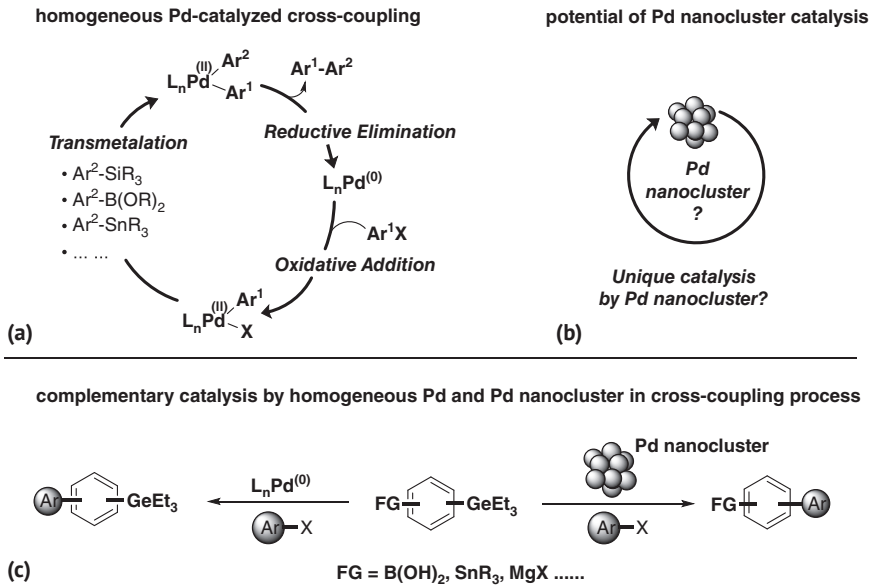

Figure 1.10 Orthogonal catalysis strategy with organogermanes based on different catalytic selectivity of single palladium atoms and palladium nanoclusters.

On the one hand, the catalytic products present selectivity toward different metal species. On the other hand, the metal nanocluster catalysts are selective to the reactions. Lee and coworkers found that gold nanoclusters demonstrated selectivity toward the CO oxidation reaction [47]. They designed the experiment of room-temperature CO oxidation on planar model Au_n/TiO_2 catalysts prepared by deposition of size-selected Au_n^+ nanoclusters, in which $n = 1, 2, 3, 4, 7$. The catalytic activity of gold nanoclusters have been found to be strongly dependent on deposited nanocluster size, with substantial activity for Au_n as small as three gold atoms.

No matter product selectivity or catalyst selectivity, metal nanocluster catalysis provide a route to control pathways of the reactions, thus furnishing valuable and desired products that are difficult to be achieved by other catalytic methods.

1.5 Metal Nanocluster Catalysis: Mechanism

Catalysis is a dynamic process, in which the single metal atoms, metal nanoclusters, and metal nanoparticles are all possibly involved. As the bridging point of the monoligated metal species (or metal salt) and the metal nanoparticle, metal nanocluster (especially with atomically precise structures) constitutes the key intermediate for clarifying the catalytic mechanism of metal catalysis. They can be used as model catalysts to reveal the correlation between catalytic performance and catalysts structures at the atomic scale, thus being a bridge between structure and properties as well. A review paper focusing on the model catalyst role of metal nanoclusters in

catalysis is recommended, which illustrates the catalytic mechanisms in detail from theoretical and experimental perspectives [48].

We would like to take the copper-catalyzed azide-alkyne cycloaddition (CuAAC) reaction as a typical example to explain the importance of investigating the mechanism of metal catalysis by metal nanoclusters. CuAAC is one of the most famous click reactions developed by Karl Barry Sharpless, who has been awarded the 2022 Nobel Prize in Chemistry for the development of click chemistry and biorthogonal chemistry. It should be noted that this is the second time that Professor Karl Barry Sharpless was awarded the Nobel Prize in Chemistry. His first Nobel Prize came from the asymmetric catalysis in 2001. The well-recognized CuAAC reaction mechanism catalyzed by the homogeneous monoligated copper complex involves the activation of alkynes via carbon–hydrogen bond cleavage and the formation of a $\left[R{-}C{\equiv}C{-}Cu\right]$ intermediate (Figure 1.11). The fact that internal alkynes are generally unreactive to azides in the presence of copper complexes further verifies this catalytic mechanism. On the other hand, it has been found that some heterogeneous copper catalysts were able to catalyze the AAC reaction with the internal alkyne as the substrate. As a result of the polydispersity and the imprecise structures of the heterogeneous copper catalysts, their catalytic mechanism is mysterious. Copper nanoclusters that fall into the critical point between copper atoms and copper nanoparticles provide an opportunity to understand the catalytic mechanism of CuAAC reactions under heterogeneous conditions. Fang and coworkers synthesized an Au_4Cu_4 nanocluster with the composition of $[Au_4Cu_4(dppm)_2(SAdm)_5]Br$ (dppm = bis(diphenylphosphino)methane; SAdm = adamantane-1-thiolate) [49]. This nanocluster has robust structure and its composition and structure can be well characterized by ESI-MS and single-crystal X-ray diffraction of (SCXRD). Zhu and coworkers found that Au_4Cu_4 nanocluster not only catalyzed the click reaction of azides and terminal alkynes but also smoothly catalyzed the click reaction between azides and internal alkynes. Based on the specific and repeatable ultraviolet and visible (UV–vis), ESI-MS, nuclear magnetic resonance (NMR), Fourier-transform infrared (FT-IR), and XPS spectra, they conducted the in-depth mechanism investigation on

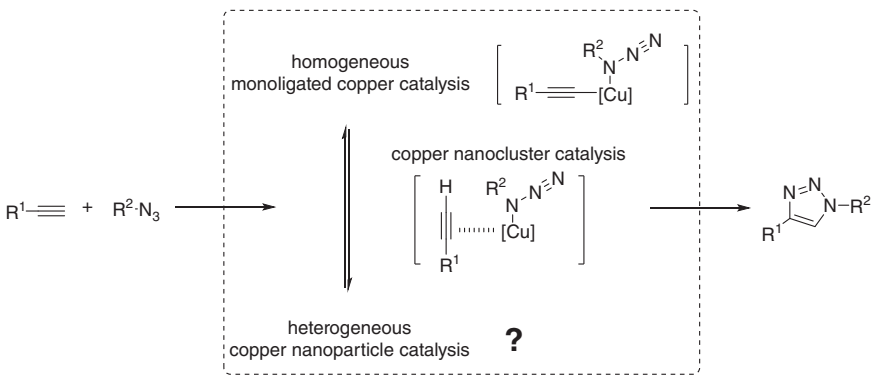

Figure 1.11 Activation modes of CuAAC click reaction catalyzed by different types of metal species.

the Au_4Cu_4-catalyzed AAC reaction. A crucial intermediate [Au_4Cu_4-π-(R—C≡C—H] was observed by thin-layer chromatography (TLC) and further captured and structurally determined by ESI-MS. This intermediate demonstrates that Au_4Cu_4 activates alkynes by π-activation instead of deprotonation (Figure 1.11). This study reveals the alternative reaction pathway of CuAAC reaction under heterogeneous reaction conditions, with the copper metal nanocluster catalysis as a case study.

Another representative case is the metal-catalyzed hydrogenation reactions. Although there are many proposed mechanisms toward metal-catalyzed hydrogenations, the generally recognized key steps for homogeneous and heterogeneous catalytic conditions are the noncovalent ligand–substrate interaction and adsorption of substrates on the metal surface, respectively. For the monoligated metal species catalyzed hydrogenation, the molecular interactions between the unsaturated substrate, hydrogen gas, and the ligand are able to be well-defined by characterizations such as NMR, MS, and SCXRD because of the atomically precise structure of the catalyst [50–52]. For the heterogeneous catalysis, the adsorption of substrates and hydrogen gas, and the desorption of the hydrogenated product are generally considered to be the rate-determining steps (RDS). As a result of the relatively weak molecular interactions between surface ligand and the substrate, the control of selectivity under heterogeneous hydrogenation conditions is challenging. This problem is also partially attributed to the imprecise structure of the heterogeneous catalysts, which make it difficult to reveal the real processes during heterogeneous hydrogenation reactions [53, 54]. Metal nanoclusters with atomically precise structures would be ideal model catalysts for investigating the detailed catalytic processes of heterogeneous hydrogenation reactions. An early work from Zhu and coworkers revealed that the activation of C═O group at the icosahedral Au_{13} core and the activation of hydrogen gas at the outer Au_{12} surface are the key factors for the high efficiency of $Au_{25}(SR)_{18}$-catalyzed selective hydrogenation of α,β-unsaturated ketones and aldehydes [55]. This proposed catalytic model would be very helpful for the further structural design of catalytically active heterogeneous hydrogenation catalysts.

For the classic cross-coupling reaction, the catalytic mechanisms might be different as well by using monoligated metal complexes and metal nanoclusters as catalysts, respectively. For example, oxidative addition, transmetallation, and reductive elimination are the basic element reactions for the conventional Pd^0-catalyzed Suzuki reaction (Figure 1.12a). However, for palladium nanocluster that is composed of three palladium atoms, the catalytic process has been verified via a direct ligand exchange between the halogen atoms and the aryl group of the organoboronic acid (Figure 1.12b). The newly developed route of Suzuki reaction via palladium nanocluster catalysis is even more efficient than the typical monoligated palladium catalysis [56, 57]. Based on the previous reports, the heterogeneous palladium-catalyzed cross-coupling reactions possess significantly high turnover numbers under certain conditions. The results suggest that more efficient catalytic process might be involved during these heterogeneous metal-catalyzed cross-coupling reactions.

Apart from the distinct catalytic mechanisms involved in metal nanocluster catalysis, the methods for investigating the mechanisms of molecular homogeneous

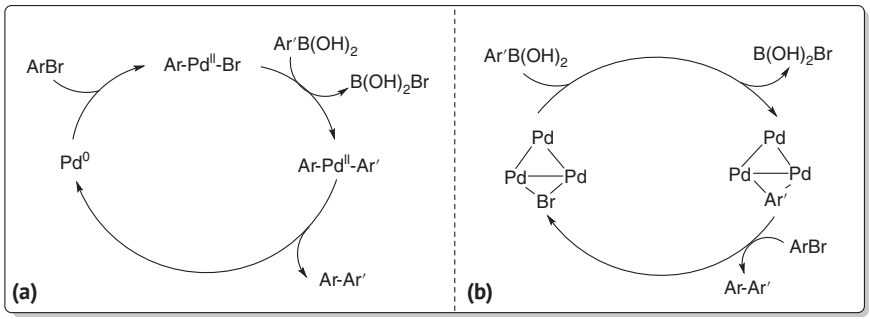

Figure 1.12 (a) Conventional Pd^0-catalyzed Suzuki reaction. (b) Palladium nanocluster-catalyzed Suzuki reaction.

catalysis, heterogeneous catalysis and nanocluster catalysis are different as well. Detection and capture of intermediates, kinetic experiments, and simulation based on molecular structures are the powerful tools for revealing the catalytic mechanisms of molecular homogeneous catalysts. For heterogeneous catalysis, the first thing that should be confirmed is the real catalytic species because of the "cocktail"-type systems [58, 59] during heterogeneous catalysis as we mentioned in Section 1.2. After confirming the heterogeneous pathway, characterizations such as XPS and extended X-ray absorption fine structure (EXAFS) are usually employed for exploring the catalytic mechanism. Owing to the fact that metal nanoclusters combine the structural features of molecular homogeneous catalysts and heterogeneous catalysts, NMR, MS, SCXRD, XPS, EXAFS, etc. are all practical tools for revealing the catalytic processes of metal nanocluster catalysis. Nevertheless, clearly identifying the whole catalytic cycle of metal nanocluster catalysts is still a challenging task as a result of their dynamic transformations during catalysis compared to monoligated metal catalysts.

References

1 F. Meemken, A. Baiker, Recent Progress in Heterogeneous Asymmetric Hydrogenation of C═O and C═C Bonds on Supported Noble Metal Catalysts. *Chem. Rev*. **2017**, *117*, 11522–11569.

2 A. Fürstner, P. W. Davies, Catalytic Carbophilic Activation: Catalysis by Platinum and Gold π Acids. *Angew. Chem. Int. Ed*. **2007**, *46*, 3410–3449; Katalytische carbophile Aktivierung: Platin- und Gold-p-Säuren als Katalysatoren. *Angew. Chem*. **2007**, *119*, 3478–3519.

3 Ł. Banach, P. A. Guńka, J. Zachara, W. Buchowicz, Half-Sandwich Ni(II) Complexes [Ni(Cp)(X)(NHC)]: From an Underestimated Discovery to a New Chapter in Organonickel Chemistry. *Coord. Chem. Rev*. **2019**, *389*, 19–58.

4 J. Thongpaen, R. Manguin, O. Baslé, Chiral N-Heterocyclic Carbene Ligands Enable Asymmetric C—H Bond Functionalization. *Angew. Chem. Int. Ed*. **2020**, *59*, 2–12; *Angew. Chem*. **2020**, *132*, 10326–10335.

5 Y. Wang, H. Arandiyan, J. Scott, A. Bagheri, H. X. Dai, R. Amal, Recent Advances in Ordered Meso/Macroporous Metal Oxides for Heterogeneous Catalysis: A Review. *J. Mater. Chem. A*. **2017**, *5*, 8825–8846.

6 B. Su, J. F. Hartwig, Development of Chiral Ligands for the Transition-MetalCatalyzed Enantioselective Silylation and Borylation of C—H Bonds. *Angew. Chem. Int. Ed*. **2021**, *60*, 2–16; *Angew. Chem*. **2022**, *134*, e202113343.

7 Y. Dong, G. Goubert, M. N. Groves, J.-C. Lemay, B. Hammer, P. H. McBreen, Structure and Dynamics of Individual Diastereomeric Complexes on Platinum: Surface Studies Related to Heterogeneous Enantioselective Catalysis. *Acc. Chem. Res*. **2017**, *50*, 1163–1170.

8 M.-A. Légaré, G. Bélanger-Chabot, R. D. Dewhurst, E. Welz, I. Krummenacher, B. Engels, H. Braunschweig, Nitrogen Fixation and Reduction at Boron. *Science* **2018**, *359*, 896–900.

9 J. Twilton, M. Christensen, D. A. DiRocco, R. T. Ruck, I. W. Davies, D. W. C. MacMillan, Selective Hydrogen Atom Abstraction Through Induced Bond Polarization: Direct a-Arylation of Alcohols Through Photoredox, HAT, and Nickel Catalysis. *Angew. Chem. Int. Ed*. **2018**, *57*, 5369–5373; *Angew. Chem*. **2018**, *130*, 5467–5471.

10 A. Ruffoni, C. Hampton, M. Simonetti, D. Leonori, Photoexcited Nitroarenes for the Oxidative Cleavage of Alkenes. *Nature* **2022**, *610*, 81–86.

11 F. A. Cotton, Strong Homonuclear Metal-Metal Bonds. *Acc. Chem. Res*. **1969**, *2*, 240–247.

12 U. Schubert, Cluster-based Inorganic–Organic Hybrid Materials. *Chem. Soc. Rev*. **2011**, *40*, 575–582.

13 R. Jin, C. Zeng, M. Zhou, Y. Chen, Atomically Precise Colloidal Metal Nanoclusters and Nanoparticles: Fundamentals and Opportunities. *Chem. Rev*. **2016**, *116*, 10346–10413.

14 Q. Liu, X. Wang, X. Wang, Sub-1 nm Materials Chemistry: Challenges and Prospects. *J. Am. Chem. Soc*. **2024**, *146*, 26587–26602.

15 I. Chakraborty, T. Pradeep, Atomically Precise Clusters of Noble Metals: Emerging Link between Atoms and Nanoparticles. *Chem. Rev*. **2017**, *117*, 8208–8271.

16 D. J. Cole-Hamilton, Homogeneous Catalysis-New Approaches to Catalyst Separation, Recovery, and Recycling. *Science* **2003**, *299*, 1702–1706.

17 D. F. Chen, L. Z. Gong, Organo/Transition-Metal Combined Catalysis Rejuvenates Both in Asymmetric Synthesis. *J. Am. Chem. Soc*. **2022**, *144*, 2415–2437.

18 X. Huang, Q. Zhang, J. Lin, K. Harms, E. Meggers, Electricity-Driven Asymmetric Lewis Acid Catalysis. *Nat. Catal*. **2018**, *2*, 34–40.

19 D. A. Nicewicz, D. W. C. MacMillan, Merging Photoredox Catalysis with Organocatalysis: The Direct Asymmetric Alkylation of Aldehydes. *Science* **2008,** *322*, 77–80.

20 X. F. Wu, P. Anbarasan, H. Neumann, M. Beller, From Noble Metal to Nobel Prize: Palladium-Catalyzed Coupling Reactions as Key Methods in Organic Synthesis. *Angew. Chem. Int. Ed*. **2010**, *49*, 9047–9050; *Angew. Chem*. **2010**, *122*, 9231–9234.

21 J. Piera, J.-E. Bäckvall, Catalytic Oxidation of Organic Substrates by Molecular Oxygen and Hydrogen Peroxide by Multistep Electron Transfer—A Biomimetic Approach. *Angew. Chem. Int. Ed*. **2008**, *47*, 3506–3523; *Angew. Chem*. **2008**, *120*, 3558–3357.

22 B. Qiao, A. Wang, X. Yang, L. F. Allard, Z. Jiang, Y. Cui, J. Liu, J. Li, T. Zhang, Single-Atom Catalysis of Co Oxidation Using Pt_1/FeO_x. *Nat. Chem*. **2011**, *3*, 634–641.

23 L. N. Chen, K. P. Hou, Y. S. Liu, Z. Y. Qi, Q. Zheng, Y. H. Lu, J. Y. Chen, J. L. Chen, C. W. Pao, S. B. Wang, Y. B. Li, S. H. Xie, F. D. Liu, D. Prendergast, L. E. Klebanoff, V. Stavila, M. D. Allendorf, J. Guo, L. S. Zheng, J. Su, G. A. Somorjai, Efficient Hydrogen Production from Methanol Using a Single-Site Pt_1/CeO_2 Catalyst. *J. Am. Chem. Soc*. **2019**, *141*, 17995–17999.

24 Y. Zhang, S. Pang, Z. Wei, H. Jiao, X. Dai, H. Wang, F. Shi, Synthesis of a Molecularly Defined Single-Active Site Heterogeneous Catalyst for Selective Oxidation of N-Heterocycles. *Nat. Commun*. **2018**, *9*, 1465.

25 J. L. Sun, H. Jiang, P. H. Dixneuf, M. Zhang, Multicomponent Reductive Coupling for Selective Access to Functional γ-Lactams by a Single-Atom Cobalt Catalyst. *J. Am. Chem. Soc*. **2024**, *146*, 11289–11298.

26 P. Ryabchuk, G. Agostini, M.-M. Pohl, H. Lund, A. Agapova, H. Junge, K. Junge, M. Beller, Intermetallic Nickel Silicide Nanocatalyst—A Non-noble Metal–based General Hydrogenation Catalyst. *Sci. Adv*. **2018**, *4*, eaat0761.

27 A. Balanta, C. Godard, C. Claver, Pd Nanoparticles for C—C Coupling Reactions. *Chem. Soc. Rev*. **2011**, *40*, 4973–4985.

28 A. T. Bell, The Impact of Nanoscience on Heterogeneous Catalysis. *Science* **2003**, *299*, 1688–1691.

29 A. Bergmann, B. Roldan Cuenya, Operando Insights into Nanoparticle Transformations During Catalysis. *ACS Catal*. **2019**, *9*, 10020–10043.

30 C. Zhu, B. Yang, T. Jiang, J.-E. Bäckvall, Olefin-Directed Palladium-Catalyzed Regio- and Stereoselective Oxidative Arylation of Allenes. *Angew. Chem. Int. Ed*. **2015**, *54*, 9066–9069; *Angew. Chem*. **2015**, *127*, 9194–9197.

31 J. Piera, A. Persson, X. Caldentey, J.-E. Bäckvall, Water as Nucleophile in Palladium-Catalyzed Oxidative Carbohydroxylation of Allene-Substituted Conjugated Dienes. *J. Am. Chem. Soc*. **2007**, *129*, 14120–14121.

32 J. Liu, A. Ricke, B. Yang, J.-E. Bäckvall, Efficient Palladium-Catalyzed Aerobic Arylative Carbocyclization of Enallenynes. *Angew. Chem. Int. Ed*. **2018**, *57*, 16842–16846; *Angew. Chem*. **2018**, *130*, 17084–17088.

33 B. Yang, Y. Qiu, J.-E. Bäckvall, Control of Selectivity in Palladium(II)-Catalyzed Oxidative Transformations of Allenes. *Acc. Chem. Res*. **2018**, *51*, 1520–1531.

34 M.-B. Li, A. K. Inge, D. Posevins, K. P. J. Gustafson, Y. Qiu, J.-E. Bäckvall, Chemodivergent and Diastereoselective Synthesis of Gamma-Lactones and Gamma-Lactams: A Heterogeneous Palladium-Catalyzed Oxidative Tandem Process. *J. Am. Chem. Soc*. **2018**, *140*, 14604–14608.

35 A. M. Trzeciak, A. W. Augustyniak, The Role of Palladium Nanoparticles in Catalytic C—C Cross-Coupling Reactions. *Coord. Chem. Rev*. **2019**, *384*, 1–20.

36 A. H. M. de Vries, J. M. C. A. Mulders, J. H. M. Mommers, H. J. W. Henderickx, J. G. de Vries, Homeopathic Ligand-Free Palladium as a Catalyst in the Heck Reaction. A Comparison with a Palladacycle. *Org. Lett*. **2003**, *5*, 3285–3288.

37 J. Huang, T. Akita, J. Faye, T. Fujitani, T. Takei, M. Haruta, Propene Epoxidation with Dioxygen Catalyzed by Gold Clusters. *Angew. Chem. Int. Ed*. **2009**, *48*, 7862–7866; *Angew. Chem*. **2009**, *121*, 8002–8006.

38 M. Turner, V. B. Golovko, O. P. Vaughan, P. Abdulkin, A. Berenguer-Murcia, M. S. Tikhov, B. F. Johnson, R. M. Lambert, Selective Oxidation with Dioxygen by Gold Nanoparticle Catalysts Derived from 55-Atom Clusters. *Nature* **2008**, *454*, 981–983.

39 M. T. Reetz, J. G. de Vries, Ligand-Free Heck Reactions Using Low Pd-Loading. *Chem. Commun*. **2004**, *14*, 1559–1563.

40 A. Leyva-Perez, J. Oliver-Meseguer, P. Rubio-Marques, A. Corma, Water-Stabilized Three- and Four-Atom Palladium Clusters as Highly Active Catalytic Species in Ligand-Free C—C Cross-Coupling Reactions. *Angew. Chem. Int. Ed*. **2013**, *52*, 11554–11559; *Angew. Chem*. **2013**, *125*, 11768–11773.

41 P. J. Ellis, I. J. Fairlamb, S. F. Hackett, K. Wilson, A. F. Lee, Evidence for the Surface-Catalyzed Suzuki-Miyaura Reaction over Palladium Nanoparticles: An Operando XAS Study. *Angew. Chem. Int. Ed*. **2010**, *49*, 1820–1824; *Angew. Chem*. **2010**, *122*, 1864–1868.

42 C. Ruan, C. Meng, K. Wang, Y. Li, H. Xiang, H. Yan, W. W. Xu, M. Zhou, C. Yao, Octahedral Vs Tiara-Like $Pd_6(SR)_{12}$ Clusters. *Nano. Lett*. **2024**, *24*, 13054–13060.

43 X.-K. Wan, J.-Q. Wang, Z.-A. Nan, Q.-M. Wang, Ligand Effects in Catalysis By Atomically Precise Gold Nanoclusters. *Sci. Adv*. **2017**, *3*, e1701823.

44 D. Pun, T. Diao, S. S. Stahl, Aerobic Dehydrogenation of Cyclohexanone to Phenol Catalyzed by $Pd(TFA)_2$/2-Dimethylaminopyridine: Evidence for the Role of Pd Nanoparticles. *J. Am. Chem. Soc*. **2013**, *135*, 8213–8221.

45 D. Wang, A. B. Weinstein, P. B. White, S. S. Stahl, Ligand-Promoted Palladium-Catalyzed Aerobic Oxidation Reactions. *Chem. Rev*. **2018**, *118*, 2636–2679.

46 C. Fricke, G. J. Sherborne, I. Funes-Ardoiz, E. Senol, S. Guven, F. Schoenebeck, Orthogonal Nanoparticle Catalysis with Organogermanes. *Angew. Chem. Int. Ed*. **2019**, *58*, 17788–17795; *Angew. Chem*. **2019**, *131*, 17952–17959.

47 S. Lee, C. Fan, T. Wu, S. L. Anderson, CO Oxidation on Au_n/TiO_2 Catalysts Produced by Size-Selected Cluster Deposition. *J. Am. Chem. Soc*. **2004**, *126*, 5682–5683.

48 Y. Du, H. Sheng, D. Astruc, M. Zhu, Atomically Precise Noble Metal Nanoclusters as Efficient Catalysts: A Bridge between Structure and Properties. *Chem. Rev*. **2020**, *120*, 526–622.

49 Y. Fang, K. Bao, P. Zhang, H. Sheng, Y. Yun, S. X. Hu, D. Astruc, M. Zhu, Insight into the Mechanism of the CuAAC Reaction by Capturing the Crucial Au_4Cu_4-π-Alkyne Intermediate. *J. Am. Chem. Soc*. **2021**, *143*, 1768–1772.

50 J. H. Xie, S. F. Zhu, Q. L. Zhou, Transition Metal-Catalyzed Enantioselective Hydrogenation of Enamines and Imines. *Chem. Rev*. **2011**, *111*, 1713–1760.

51 L. C. Misal Castro, H. Li, J.-B. Sortais, C. Darcel, When Iron Met Phosphines: A Happy Marriage for Reduction Catalysis. *Green Chem*. **2015**, *17*, 2283–2303.

52 R. H. Morris, Exploiting Metal-Ligand Bifunctional Reactions in the Design of Iron Asymmetric Hydrogenation Catalysts. *Acc. Chem. Res*. **2015**, *48*, 1494–1502.

53 F. Zaera, Regio-, Stereo-, and Enantioselectivity in Hydrocarbon Conversion on Metal Surfaces. *Acc. Chem. Res*. **2009**, *42*, 1152–1160.

54 M. Heitbaum, F. Glorius, I. Escher, Asymmetric Heterogeneous Catalysis. *Angew. Chem. Int. Ed*. **2006**, *45*, 4732–4762; *Angew. Chem*. **2006**, *118*, 2794–2797.

55 Y. Zhu, H. Qian, B. A. Drake, R. Jin, Atomically Precise $Au_{25}(SR)_{18}$ Nanoparticles as Catalysts for the Selective Hydrogenation of α,β-Unsaturated Ketones and Aldehydes. *Angew. Chem. Int. Ed*. **2010**, *49*, 1295–1298; *Angew. Chem*. **2010**, *122*, 1317–1320.

56 F. Fu, J. Xiang, H. Chemg, L. Cheng, H. Chong, S. Wang, P. Li, S. Wei, M. Zhu, Y. Li, A Robust and Efficient Pd_3 Cluster Catalyst for the Suzuki Reaction and Its Odd Mechanism. *ACS Catal*. **2017**, *7*, 1860–1867.

57 N. Jeddi, N. W. J. Scott, I. J. S. Fairlamb, Well-Defined Pd_n Clusters for Cross-Coupling and Hydrogenation Catalysis: New Opportunities for Catalyst Design. *ACS Catal*. **2022**, *12*, 11615–11638.

58 D. B. Eremin, V. P. Ananikov, Understanding Active Species in Catalytic Transformations: From Molecular Catalysis to Nanoparticles, Leaching, "Cocktails" of Catalysts and Dynamic Systems. *Coord. Chem. Rev*. **2017**, *346*, 2–19.

59 R. H. Crabtree, Resolving Heterogeneity Problems and Impurity Artifacts in Operationally Homogeneous Transition Metal Catalysts. *Chem. Rev*. **2012**, *112*, 1536–1554.